



## **Novel optical fiber SPR temperature sensor based on MMF-PCF-MMF structure and gold PDMS film**

Yong Wang, Qing Huang, Wenjie Zhu, Minghong Yang, ELFED LEWIS

### **Publication date**

01-01-2018

### **Published in**

Optics Express;26 (2)

### **Licence**

This work is made available under the [CC BY-NC-SA 1.0](#) licence and should only be used in accordance with that licence. For more information on the specific terms, consult the repository record for this item.

### **Document Version**

1

### **Citation for this work (HarvardUL)**

Wang, Y., Huang, Q., Zhu, W., Yang, M. and LEWIS, E. (2018) 'Novel optical fiber SPR temperature sensor based on MMF-PCF-MMF structure and gold PDMS film', available: <https://hdl.handle.net/10344/6490> [accessed 23 Jul 2022].

This work was downloaded from the University of Limerick research repository.

For more information on this work, the University of Limerick research repository or to report an issue, you can contact the repository administrators at [ir@ul.ie](mailto:ir@ul.ie). If you feel that this work breaches copyright, please provide details and we will remove access to the work immediately while we investigate your claim.



# Novel optical fiber SPR temperature sensor based on MMF-PCF-MMF structure and gold-PDMS film

YONG WANG,<sup>1</sup> QING HUANG,<sup>1</sup> WENJIE ZHU,<sup>1</sup> MINGHONG YANG,<sup>1,\*</sup> ELFED LEWIS<sup>2</sup>

<sup>1</sup>National Engineering Laboratory for Fiber Optic Sensing Technology, Wuhan University of Technology, Wuhan 430070, China

<sup>2</sup>Optical Fiber Sensors Research Centre, University of Limerick, Limerick, Ireland

\*minghong.yang@whut.edu.cn

**Abstract:** In this paper, a novel optical fiber temperature sensor based on surface plasmon resonance (SPR) is presented. The sensor consists of multimode fiber-photonic crystal fiber-multimode fiber (MMF-PCF-MMF) structure coated with gold film, whose refractive index (RI) sensitivity was found to range from 1060.78 nm/RIU to 4613.73 nm/RIU in the RI range of 1.3330-1.3904. Through simulation and experimental results, the RI sensitivity of the MMF-PCF-MMF structure is found to be higher than that of multimode fiber-single mode fiber-multimode fiber (MMF-SMF-MMF) structure. The sensing area was coated with polydimethylsiloxane (PDMS) that has a high thermal coefficient, obtaining a high temperature sensitivity of  $-1.551$  nm/°C in the temperature range of 35-100 °C, which means it has a broad application prospect in medical, environmental monitoring and manufacturing industry.

© 2018 Optical Society of America under the terms of the [OSA Open Access Publishing Agreement](#)

**OCIS codes:** (060.2370) Fiber optics sensors; (310.6870) Thin films, other properties.

## References and links

1. T. K. Yadav, R. Narayanaswamy, M. H. Abu Bakar, Y. M. Kamil, and M. A. Mahdi, "Single mode tapered fiber-optic interferometer based refractive index sensor and its application to protein sensing," *Opt. Express* **22**(19), 22802–22807 (2014).
2. G. Fu, Y. Li, Q. Li, J. Yang, X. Fu, and W. Bi, "Temperature Insensitive Vector Bending Sensor based on Asymmetrical Cascading SMF-PCF-SMF Structure," *IEEE Photonics J.* **9**(3), 7103114 (2017).
3. Z. Feng, J. Li, X. Qiao, L. Li, H. Yang, and M. Hu, "A thermally annealed Mach-Zehnder Interferometer for High Temperature Measurement," *Sensors (Basel)* **14**(8), 14210–14221 (2014).
4. C. S. Park, K. I. Joo, S. W. Kang, and H. R. Kim, "A PDMS-coated optical fiber bragg grating sensor for enhancing temperature sensitivity," *J. Opt. Soc. Korea* **15**(4), 329–334 (2011).
5. W. Cui, J. Si, T. Chen, and X. Hou, "Compact bending sensor based on a fiber Bragg grating in an abrupt biconical taper," *Opt. Express* **23**(9), 11031–11036 (2015).
6. C. Markos, K. Vlachos, and G. Kakarantzas, "Bending loss and thermo-optic effect of a hybrid PDMS/silica photonic crystal fiber," *Opt. Express* **18**(23), 24344–24351 (2010).
7. M. S. Jiang, Q. M. Sui, Z. W. Jin, F. Y. Zhang, and L. Jia, "Temperature-independent optical fiber Fabry–Perot refractive-index sensor based on hollow-core photonic crystal fiber," *Optik (Stuttg.)* **125**(13), 3295–3298 (2014).
8. Q. Wang, C. Du, J. Zhang, R. Lv, and Y. Zhao, "Sensitivity-enhanced temperature sensor based on PDMS-coated long period fiber grating," *Opt. Commun.* **377**, 89–93 (2017).
9. I. Hernández-Romano, M. A. Cruz-García, C. Moreno-Hernández, D. Monzón-Hernández, E. O. López-Figueroa, O. E. Paredes-Gallardo, M. Torres-Cisneros, and J. Villatoro, "Optical fiber temperature sensor based on a microcavity with polymer overlay," *Opt. Express* **24**(5), 5654–5661 (2016).
10. M. Ding, B. Yang, P. Jiang, X. Liu, L. Dai, Y. Hu, and B. Zhang, "High-sensitivity thermometer based on single-mode-multimode FBG-singlemode fiber," *Opt. Laser Technol.* **96**, 313–317 (2017).
11. Y. Zhao, Z. Q. Deng, and H. F. Hu, "Fiber-Optic SPR Sensor for Temperature Measurement," *IEEE Trans. Instrum. Meas.* **64**(11), 3099–3104 (2015).
12. D. Brabant and W. J. Bock, "Photonic crystal fiber refractive index sensor based on surface plasmon resonance," *Proc. SPIE* **7750**, 77502K (2010).
13. C. W. Wei, C. C. Chi, L. B. Jia, Y. T. Zi, Q. T. Zhi, B. Y. Hong, M. L. Chang, and C. L. Kam, "Photonic Crystal Fiber Surface Plasmon Resonance Biosensor Based on Protein G Immobilization," *IEEE J. Sel. Top. Quantum Electron.* **19**(3), 4602107 (2013).

14. R. Jha, J. Villatoro, and G. Badenes, "Ultrastable in reflection photonic crystal fiber modal interferometer for accurate refractive index sensing," *Appl. Phys. Lett.* **93**(19), 4057–4059 (2008).
15. Y. Zhao, R. J. Tong, M. Q. Chen, and F. Xia, "Fluorescence Temperature Sensor Based on GQDs Solution Encapsulated in Hollow Core Fiber," *IEEE Photonics Technol. Lett.* **29**(18), 1544–1547 (2017).
16. Y. Li, Y. Wang, and C. Wen, "Temperature and strain sensing properties of the zinc coated FBG," *Optik (Stuttg.)* **127**(16), 6463–6469 (2006).
17. N. Irawati, S. W. Harun, H. A. Rahman, S. S. Chong, N. A. Hamizi, and H. Ahmad, "Temperature sensing using CdSe quantum dot doped poly(methyl methacrylate) microfiber," *Appl. Opt.* **56**(16), 4675–4679 (2017).

## 1. Introduction

Temperature plays a significant role in many fields, such as medical, environmental monitoring and manufacturing industry. Sensors for temperature measurement have attracted much attention in the last few years. As a relatively new type of sensor technology, optical fiber based sensors have many advantages, such as small size, high sensitivity, anti-electromagnetic interference [1, 2]. At present, there exist many kinds of structures for optical fiber temperature sensor, such as Mach-Zehnder Interferometer (MZI) [3], fiber Bragg grating (FBG) [4, 5], photonic crystal fiber (PCF) [6, 7]. Wang Qi [8] et al. have reported a PDMS-coated long-period fiber grating temperature sensor with a sensitivity of 255.4 pm/°C in the range of 20–80 °C. A Fabry-Perot configuration has also been designed for temperature sensor, whose sensitivity was 0.13 dB/°C [9]. Ding Ming [10] et al. have proposed a temperature sensor based on single mode-multimode FBG-single mode structure, achieving a temperature sensitivity of 266.25 pm/°C in the temperature range –40 °C to + 40 °C. The sensors mentioned above have made some progress in temperature. However, the intensity-modulated temperature sensor is easily affected by some factors, such as the intensity of the light source. Therefore, the wavelength-modulated sensor can better meet the actual needs.

In order to further improve the temperature sensitivity, Zhao Yong [11] et al. have reported an optical fiber temperature sensor based on the SPR principle. The optical fiber probe coated with a silver film was encapsulated into a capillary filled with alcohol to achieve enhanced sensitivity, which was a combination of the alcohol characteristic (with a high thermal coefficient) and SPR technology. The sensor showed a relatively high temperature sensitivity of 1.575 nm/°C. However, the alcohol is not easy to encapsulate, which makes the manufacturing process of this device complicated. Therefore, an optical fiber temperature sensor with simple manufacturing process and high sensitivity is needed.

In this paper, a novel optical fiber surface plasmon resonance (SPR) temperature sensor is presented which comprises a multimode fiber-photonic crystal fiber-multimode fiber (MMF-PCF-MMF) structure. The sensing area was coated with a 60 nm thickness gold film by magnetron sputtering, achieving a high refractive index (RI) sensitivity. After coating with polydimethylsiloxane (PDMS) on gold film, the optical fiber SPR temperature sensor shows a high temperature sensitivity of –1.551 nm/°C in the temperature range from 35 °C to 100 °C. Due to the simple manufacturing process and high temperature sensitivity, the novel optical fiber SPR temperature sensor based on MMF-PCF-MMF structure and gold-PDMS film may have widespread applications in the field of medical, environmental monitoring and manufacturing industry.

## 2. Sensing structure and experimental principle

The sensor consists of the MMF-PCF-MMF structure, which is shown in Fig. 1(a). At the two ends of the sensor, there are two common multimode fibers (62.5 μm core diameter and 125 μm cladding diameter). In the middle of the sensor probe, a photonic crystal fiber [Fig. 1(b)] was inserted between two multimode fibers using a standard fusion optical fiber splicer (FSM-60s, Fujikura Ltd. Japan) and an optical fiber cleaver (CT-30, Fujikura Ltd. Japan). The coating layer of the PCF was removed to expose the sensing region. Then, the sensing region was coated with a layer of 60 nm gold film by magnetron sputtering, whose microscope image is shown in Fig. 1(d).

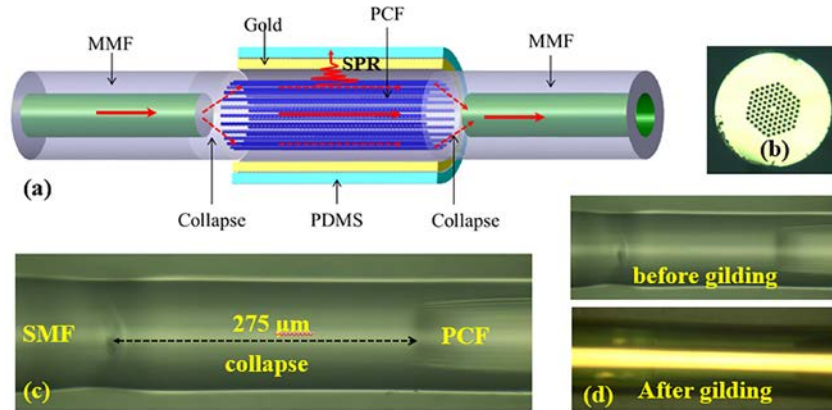


Fig. 1. (a) Multimode fiber-photonic crystal fiber -multimode fiber (MMF-PCF-MMF) structure. (b) Optical microscope image of cross section of photonic crystal fiber. (c) Optical microscope image of the junction of photonic crystal and multimode fiber. (d) Optical microscopic image of the sensing area before gilding and after gilding.

Figure 1(a) shows that the light transmitted inside the multimode fiber is limited in the core and the corresponding modes are core modes. The sensing region is a single mode PCF, whose core diameter is much smaller than that of MMF. Thus, when light is transmitted from MMF to PCF, only a small part of the light is transmitted along the core of the PCF, while the majority of the light energy is transmitted into the cladding of the PCF [12]. As shown in Fig. 1(c), there is a collapsed region at the junction of the photonic crystal fiber and multimode fiber, which can excite higher order modes to the cladding and gold film interface [13].

The light is totally reflected at the interface between the cladding and the gold film, since the thickness of the metal thin film is smaller than the depth of penetration of the evanescent wave, there is still an evanescent wave at the boundary between the outer side of the metal film and the medium. The component of the wave vector interface is:

$$K_z = \frac{\omega}{c} \sqrt{\epsilon_0} \sin \theta \quad (1)$$

where  $\omega$  is the angular frequency of the incident light,  $c$  is the speed of light,  $\epsilon_0$  is the dielectric constant of the cladding, and  $\theta$  is the angle of incidence.

At the interface between the film and the ambient medium, the plasma oscillation confined to the metal surface produces an electromagnetic wave propagating in the Z-direction and whose amplitude is attenuated in the Z-direction, which is called the surface plasmon wave. The wave vector is:

$$K_{spw} = \text{Re} \left[ \frac{\omega}{c} \sqrt{\frac{\epsilon_1 \epsilon_2}{\epsilon_1 + \epsilon_2}} \right] \quad (2)$$

where  $\epsilon_1$  is the dielectric constant of the metal film,  $\epsilon_2$  is the dielectric constant of dielectric material on the metal film.

When  $K_z = K_{spw}$ , surface plasmon resonance absorption occurs, the intensity of the reflected light decreases to a minimum, and the resonant absorption peak appears in the spectrum. The wavelength of the incident light is called the resonant wavelength of SPR. By measuring the change of the resonant wavelength, the relationship between the refractive index of the surface of the metal film and the resonance wavelength can be obtained. Since the resonant wavelength is very sensitive to the change in the refractive index of the surrounding environment, the SPR sensor has a high refractive index (RI) sensitivity.

Due to the high thermal coefficient of the PDMS material, the RI of PDMS varies with temperature [9]. It is therefore feasible to develop an optical fiber temperature sensor based on surface plasmon resonance by combining PDMS and SPR technology. In experimental, PDMS mixed with the curing agent (Sylgard 184) at the ratio of 10:1 was stirred for 10 minutes. The mixture was then enclosed in the vacuum pumping device to remove any air bubbles. After that, sensing region was coated with PDMS and heated at 80 °C for 2 hours. The novel optical fiber SPR temperature sensor based on MMF-PCF-MMF structure and gold-PDMS film was therefore fabricated in a relatively simple manner.

### 3. Results and discussions

#### 3.1 Study of the optimal PCF length

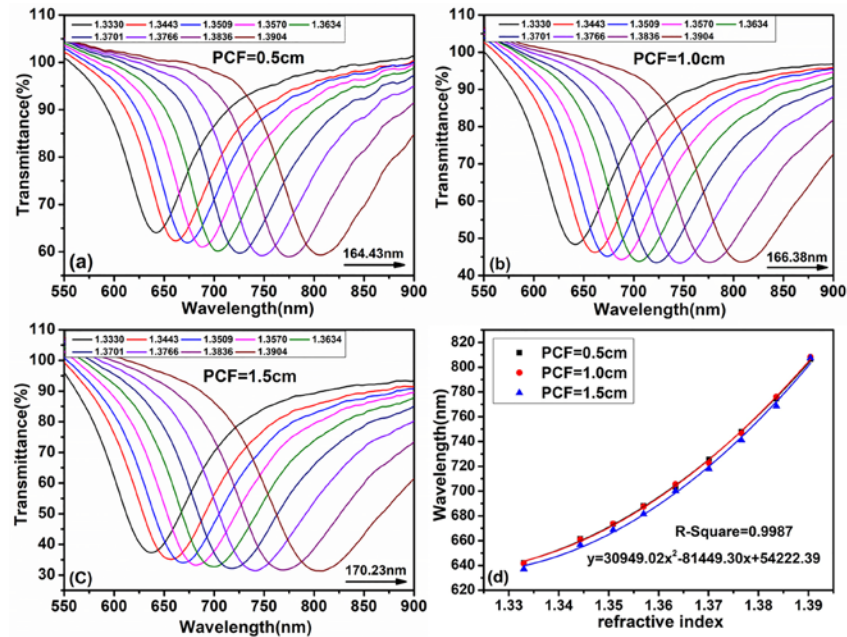


Fig. 2. Normalized transmission spectra of three sensors with different photonic crystal fiber length ((a) 0.5 cm, (b) 1.0 cm, (c) 1.5 cm) in different glycerol concentrations. (d) The relation spectra between the wavelength and refractive index of three sensors with different photonic crystal fiber length.

As can be seen in Fig. 2, the influence of different PCF lengths on sensor performance was investigated. Figures 2(a)-2(c) show the SPR spectra for three different photonic crystal fiber lengths (0.5 cm, 1.0 cm and 1.5 cm) at different concentrations of glycerol whose mass concentrations are 0%, 10%, 15%, 20%, 25%, 30%, 35%, 40% and 45%, respectively. The corresponding refractive indexes are 1.3330, 1.3443, 1.3509, 1.3570, 1.3634, 1.3701, 1.3766, 1.3836 and 1.3904, respectively. And the SPR spectra of the three sensors show a pronounced redshift in the RI range of 1.3330 to 1.3904, whose wavelength shifts are 164.43 nm, 166.38 nm and 170.23 nm, respectively. From Fig. 2(d), it can be observed that there is a repeatable relationship between the wavelength shift and the refractive index. The three curves almost coincide, which proves that the length of the photonic crystal fiber has little or no influence on the RI sensitivity of the sensor. Moreover, the RI sensitivity of the sensor increases with the increase of refractive index, which is found to range from 1060.78 nm/RIU to 4613.73 nm/RIU in the RI range of 1.3330-1.3904. It has been previously reported that photonic crystal fibers have potential applications for high accuracy refractive index measurement [14] and the measurements recorded in Fig. 2 (d) confirm this.



Figure 3 shows the transmission spectra of three different sensors with a PCF length of 0.5 cm, 1.0 cm and 1.5 cm recorded at a refractive index of 1.3904. The center wavelengths of the dip in the case of the three different sensors are 806.53 nm, 808.11 nm and 807.40 nm, respectively, which indicates that the resonance wavelength of the SPR is independent of the PCF length. However, the dip width and the dip losses increase as the length of PCF increases. The purpose of this work is to find an optimal PCF length of the sensor for temperature monitoring, and based on the results of Fig. 3, the sensor with a PCF length of 1.0 cm shows the best combination of dip width and dip losses. At the same time, the blind increase of the length of the sensor is not conducive to the application of the sensor, the shorter the length, the greater the error caused by cutting, thus making 1 cm-long PCF most suitable for fabricating the temperature sensor.

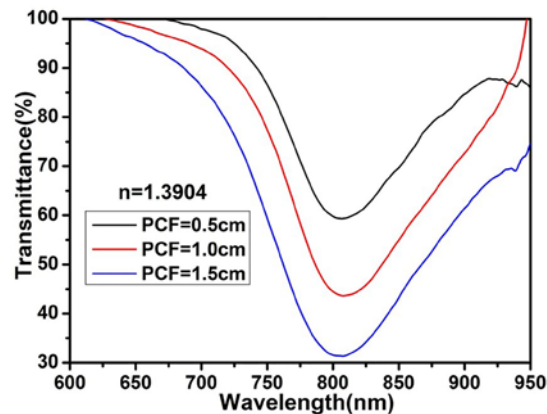


Fig. 3. Normalized transmission spectra in the RI of 1.3904 for different photonic crystal fiber length.

### 3.2 Comparison of MMF-PCF-MMF and MMF-SMF-MMF structure

The use of PCF between two multimode optical fibers as a sensing region is more effective than single mode fiber (SMF) to stimulate SPR. A numerical analysis in COMSOL shows that the fundamental modes of SMF and PCF can be well bound in the core region, while the cladding pattern of PCF is quite different from SMF, as shown in Fig. 4. The simulation wavelength was set to 750 nm, the square blue area represents the PDMS and the outer edge of the fiber is a layer of 60 nm gold film. The refractive indexes of PDMS, PCF, SMF-core and SMF-cladding were set to 1.4, 1.4546, 1.4679, 1.4613, respectively. And the refractive index of gold film was set to  $0.63869 + 4.3601i$ . As the thickness of the gold film is very thin and more emphasis is given to the cladding mode to stimulate the SPR, it is reasonable to neglect the effect of the gold film in the analysis, and focus on the mode distribution of the cladding mode. The second-order mode field was selected for analysis. The simulation results show that the effective RIs of the fundamental mode and the cladding mode of the SMF are 1.4646432 and 1.4612483, respectively. The effective RI of the fundamental mode of the SMF is greater than the effective RI of the cladding mode, which are both greater than the RI of the PDMS. Combined with the mode field distribution of SMF [Fig. 4(b)], the energy of the cladding mode is more concentrated in a position near the core. However, the silica cladding on the outside of the PCF air hole forms a high refractive index ring, so that the energy of the high-order cladding mode is concentrated in the vicinity of the gold film, as shown in Fig. 4(a). The simulation results show that the effective RIs of the high refractive index ring and the fundamental mode of the PCF are 1.4573572 and 1.4559824, respectively. The effective RI of the high refractive index ring of the PCF is greater than the fundamental mode, which are both greater than the RI of the PDMS, so PCF can stimulate a stronger SPR and improve the RI sensitivity of the sensor.

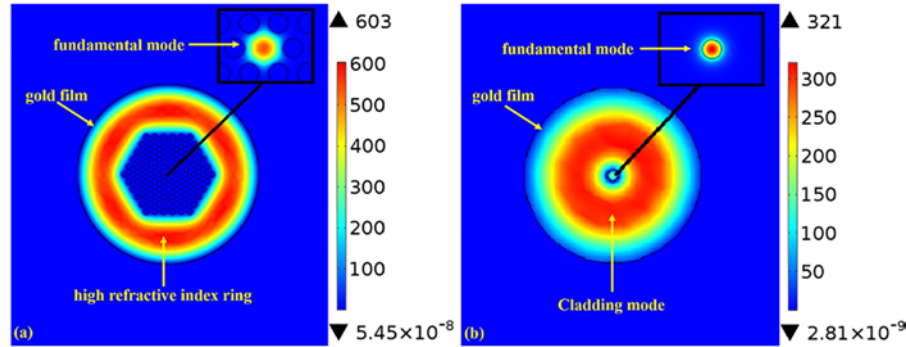


Fig. 4. (a) The mode field of photonic crystal fiber. (b) The mode field of single mode fiber.

In addition, the simulation results were verified by comparison with the experimental results. The same length (1.0 cm) of PCF and SMF were selected as the sensing area. Firstly, both the MMF-PCF-MMF structure and MMF-SMF-MMF structure were coated with a 60 nm thickness gold film by magnetron sputtering, and the RI sensitivity differences between the two sensors were investigated. From Fig. 5, both the MMF-PCF-MMF structure and the MMF-SMF-MMF structure show a clear red shift when the refractive index changes from 1.3330 to 1.3904, whose wavelength shift are 166.38 nm and 137.73 nm, respectively. There is also a consistent curve relationship in each case between the wavelength shift and the refractive index, as shown in Fig. 6. The RI sensitivity of the MMF-PCF-MMF structure is higher than that of the MMF-SMF-MMF structure. For the RI value of 1.3904, the sensitivity of the MMF-PCF-MMF structure (4613.73 nm/RIU) is higher than that of the MMF-SMF-MMF structure (3471.46 nm/RIU).

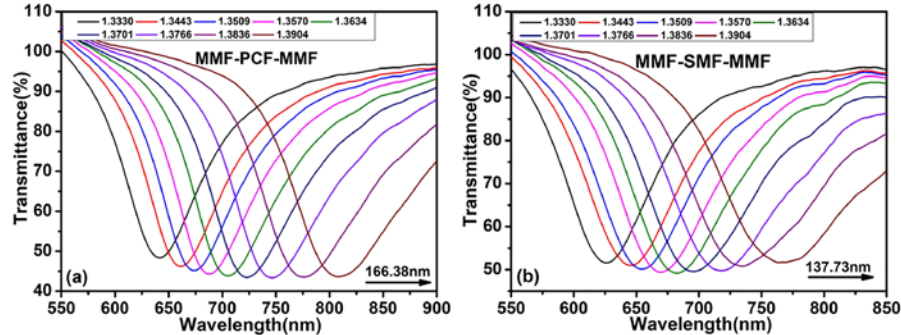


Fig. 5. (a) Normalized transmission spectra of MMF-PCF-MMF structure in different glycerol concentrations. (b) Normalized transmission spectra of MMF-SMF-MMF structure in different glycerol concentrations.

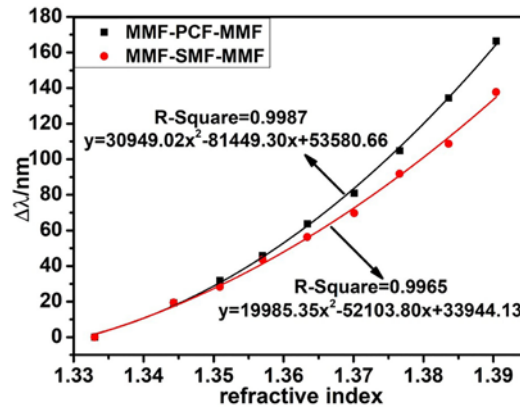


Fig. 6. The relation spectra between the wavelength and refractive index of MMF-PCF-MMF structure and MMF-SMF-MMF structure.

### 3.3 Temperature sensing

The experimental interrogation system for the optical fiber SPR temperature sensor is shown schematically in Fig. 7. Broadband light is delivered from the halogen lamp (12 mW, HL-2000, Ocean Optic Co.) and produces an SPR effect in the sensing region. The temperature-controlled chamber controls the temperature change of the sensing region. The SPR spectrum is received using an optical fiber spectrometer (Flame-T-VIS-NIR, Ocean Optic Co.) and recorded using a spectroscopy software (Ocean Optic Co.).

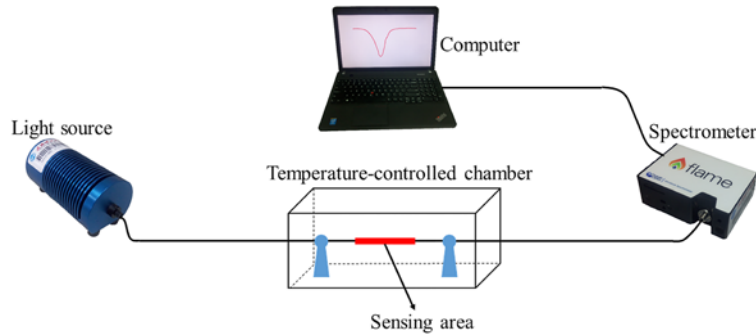


Fig. 7. Schematic diagram of the experimental setup.

Due to its high thermal coefficient, PDMS was coated on the sensing region of the sensor with a PCF length of 1.0 cm, which facilitated the temperature measurement. In order to evaluate the temperature measurement results of the sensor more accurately, 30 °C was used as the reference spectrum and spectral changes were measured as changes from this value. The experimental results are shown in Fig. 8. Figure 8(a) shows a clear blue shift of the wavelength with the increase of temperature, which is the result of the decreasing refractive index of PDMS as the temperature increases. The wavelength shift is 99.40 nm in the temperature range of 35-100 °C.

Figure 8(b) exhibits a good linear relationship ( $R\text{-square} = 0.9977$ ) between wavelength and temperature, which can be expressed as:

$$y = -1.551x + 948.086 \quad (3)$$

where  $y$  represents the wavelength (nm) and  $x$  represents the temperature of the environment (°C). The temperature sensitivity of the sensor is  $-1.551 \text{ nm/}^\circ\text{C}$ . As shown in Table 1,



compared with many reported optical fiber sensors, the sensor has a high temperature sensitivity [8, 11, 16, 17].

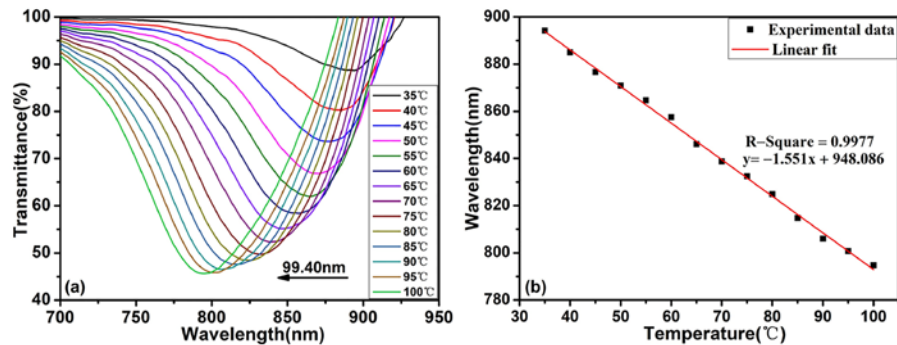


Fig. 8. (a) Normalized transmission spectra of the sensor in different temperature. (b) Relation spectra between resonance wavelength and temperature.

Table 1. Comparison of optical fiber sensor for temperature sensing.

Type	Year	Sensitivity (pm/°C)	T range (°C)	Sensitization method
LPFG [8]	2016	255.4	20-80	PDMS
SPR [11]	2015	1574.5	35-70	anhydrous ethanol
HCF [15]	2017	123.7	10-80	Graphene quantum dots
FBG [16]	2016	49.6	35-80	zinc
PMF [17]	2017	58.5	25-48	CdSe quantum dot
In this paper	2018	1551	35-100	Gold-PDMS

#### 4. Conclusion

In conclusion, a novel optical fiber SPR temperature sensor has been designed and fabricated based on MMF-PCF-MMF structure coated with a gold-PDMS film. The influence of including the PCF on sensor performance has been evaluated experimentally and in simulation. It was determined that the length of the PCF had no influence on the refractive index sensitivity of the sensor, but affected the dip width and the dip losses. The refractive index sensitivity of the sensor was found to range from 1060.78 nm/RIU to 4613.73 nm/RIU in the RI range of 1.3330-1.3904 and when compared with the MMF-SMF-MMF structure, the MMF-PCF-MMF structure exhibits a higher refractive index sensitivity. After coating with PDMS on gold film, the newly formed temperature sensor achieved a high sensitivity ( $-1.551$  nm/°C), which may find widespread application in many fields, including medical, environmental monitoring and manufacturing industry.

#### Acknowledgment

This work was supported by the National Natural Science Foundation of China (NO. 61575151).